Rev.Adv.Mater.Sci. 18(2008) 112-120

SURFACE CHARACTERISTICS OF NITROGEN AND ARGON PLASMA IMMERSION ION IMPLANTATION OF Cu-Zr-Al BULK METALLIC ALLOY

T. L. Cheung and C. H. Shek

Department of Physics and Materials Science, City University of Hong KongTat Chee Avenue, Kowloon, Hong Kong

Received: March 29, 2008

Abstract. Plasma Immersion ion implantation (PIII) offers a technique for metallic glasses to improve the surface properties. The $(Cu_{50}Zr_{50})_{92}Al_8$ bulk metallic glass (BMG) has relatively high glass forming ability (GFA), it is chosen for surface modification experiment. The influences of nitrogen and argon ion implantation on $(Cu_{50}Zr_{50})_{92}Al_8$ BMG were investigated. After PIII, the surfaces of implanted samples remain amorphous except that ZrO_2 formed on the surface. We observed Cu and Al segregation beneath the top oxide layer after ion implantation.

1. INTRODUCTION

In recent years, it is known that metallic glasses have attractive physical and chemical characteristics such as high strength, hardness, toughness and high corrosion resistance [1]. In order to use the metallic glass in practical engineering applications, the resistance to environmental attack should also be enhanced. Due to this reason, there is a need of studying surface modification of metallic glasses. PIII is a fast, cost-effective method which can be used for modifying the surface properties of many materials [2,3]. PIII offers a plasma treatment in which the ion energy can be adjusted. By choosing proper duty cycle and sample cooling or heating, PIII can be conducted at designated working conditions. During PIII, surface absorption and implantation as well as diffusion will take place simultaneously on the surface with a non-line-of-sight characteristic [4]. There does not exist any abrupt interface and film delamination is much less serious for an ion implanted surface when compare to coating. Plasma treated surface has been shown to enhance the hardness and wear resistance of other materials without degrading the corrosion resistance [4,5].

Previous paper has been revealed that among $(Cu_{50}Zr_{50})_{100-x}Al_x$ BMGs system (x = 0 and $3 \leq x \leq 10$ at.%) [6,7], the best GFA accompanied with good mechanical properties was found at x = 8. Hence the $(Cu_{50}Zr_{50})_{92}Al_8$ BMG is chosen to perform the surface modification experiments. The influences of nitrogen and argon pulsed ion implantation with implantation voltages of 40 kV on $(Cu_{50}Zr_{50})_{92}Al_8$ BMG were investigated. The effect of PIII on surface properties has been widely studied in many kinds of materials but seldom been explored in BMGs. The aim of the present study is to investigate the effect of PIII on the surface structure of Cu-Zr-Al BMG.

2. EXPERIMENTAL PROCEDURE

Alloy ingots of nominal compositions $(Cu_{50}Zr_{50})_{92}Al_8$ were prepared by arc melting mixtures of pure metals with purities above 99.9% under a Ti-gettered argon atmosphere. Each ingot was remelted four times and cast by suction of the melt

Corresponding author: C. H. Shek, e-mail: apchshek@cityu.edu.hk

© 2008 Advanced Study Center Co. Ltd.

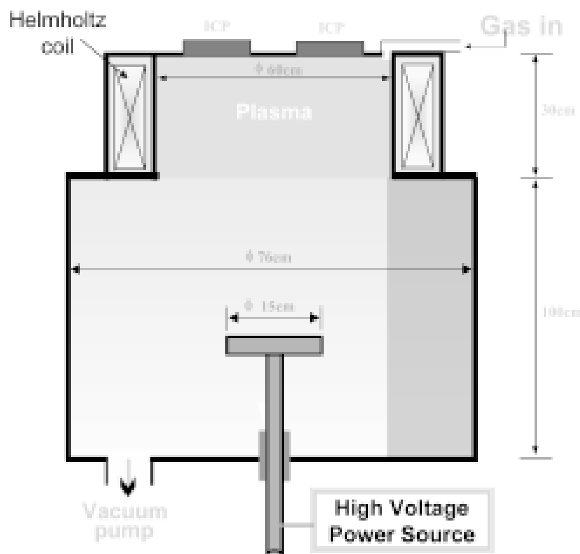

Fig. 1. Schematic diagram of the plasma immersion ion implantation instrument.

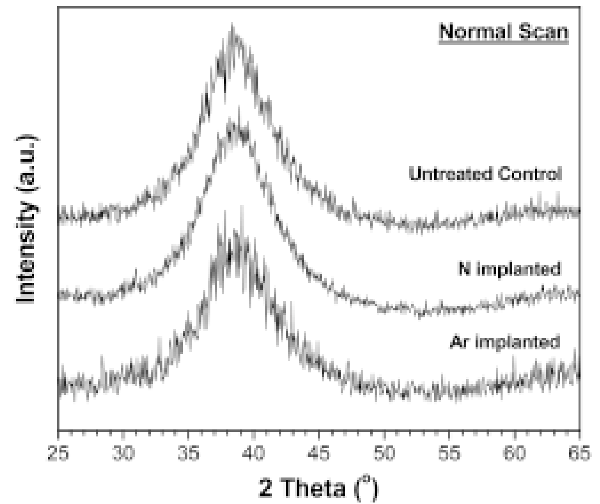

Fig. 2. XRD spectra of the untreated control, nitrogen and argon implanted $(Cu_{50}Zr_{50})_{92}Al_8$ samples with normal (θ-2θ) scan mode in the range of 2θ = 25° to 65°.

into a copper mold to obtain a 50 mm-long and 3 mm diameter cylindrical rod. The transverse cross-sections of the as-cast samples were analyzed with Siemens D500 X-ray diffractometer (XRD) with Cu K_α radiation source (λ = 1.5406 Å). The thermal properties of the as-cast samples were measured diffraction scanning calorimeter (DSC) with a Perkin Elmer DSC 7 under a purified nitrogen atmosphere at a constant heating rate of 20 K/min. PIII of as-cast $(Cu_{50}Zr_{50})_{92}Al_8$ samples were performed with radio-frequency (RF), by the inductively coupled plasma (ICP) plasma immersion ion implanter in the Plasma Laboratory of the City University of Hong Kong [8]. A Schematic diagram of the equipment is shown in Fig. 1. Prior to ion implantation, Argon ion sputter cleaning was conducted on the samples at 500 V for 5 minutes in the form of direct current. Nitrogen and argon ion implantations in the samples were conducted using a pulsed bias of 40 kV for 1 hour. The frequency and pulse width were 30 μs and 200 Hz, respectively. During the PIII experiment, the working pressure was kept at $5{\cdot}10^{-4}$ Torr. The bulk amorphous structure of the implanted BMGs samples were confirmed with Siemens D500 XRD and Perkin Elmer DSC 7. Grazing incidence X-ray diffraction (GIXRD) measurements were performed with a Bruker D8 Advance XRD equipped in the Chemistry Department of the University of Hong Kong. The GIXRD uses Cu *K* (alpha1, 2) radiation (λ=1.5406 Å). The elemental depth profiles and chemical states were determined by X-ray photoelectron spectroscopy (XPS) using an ULVAC-PHI 5802 system electron spectrometer installed with a monochromatized Al K_α radiation (1486.6 eV).

3. RESULTS AND DISCUSSIONS

The XRD spectra of the untreated control, nitrogen and argon implanted samples with normal (symmetric θ-2θ Bragg-Brentano) XRD scan mode in the range of 2θ = 25° to 65° are shown in Fig. 2. Broad diffuse peaks without substantial sharp peak are observed in the spectra of the control and the ion implanted samples, indicating that the bulk of the implanted samples remain its amorphous state.

Fig. 3 shows the GIXRD spectra for the control, nitrogen and argon ion implanted samples, respectively. The surfaces of the implanted samples are detected by grazing incidence angle of 1°. It can be seen that, on top of the amorphous diffuse halo, there are three obvious peaks around 2θ = 30.3°, 50.4°, and 60.2° for nitrogen and argon ion implantation samples. The samples after two types of ion implantation are mixtures of a small amount of crystallites and amorphous material. The main peaks agree well with zirconium dioxide (ZrO_2) phase. The presence of surface oxides after nitrogen and argon ion implantation is attributed to the existence of some residual oxygen in the implan-

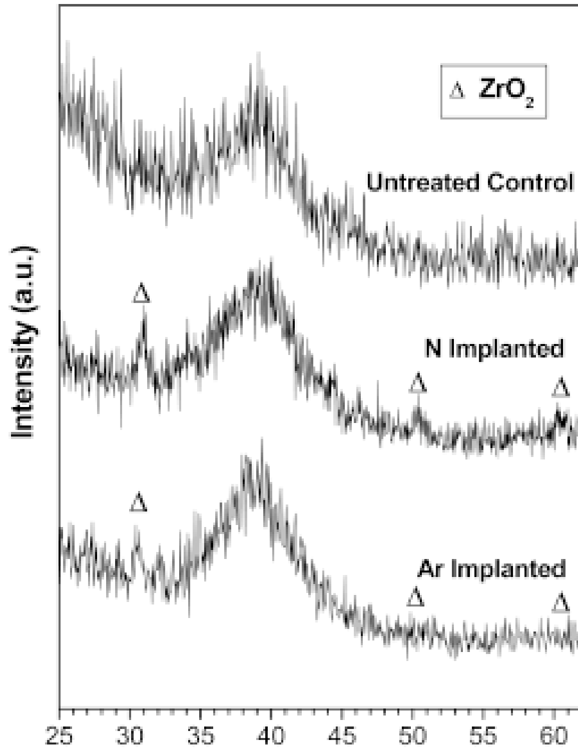

Fig. 3. GIXRD spectra for the (a) control and (b) nitrogen and (c) argon ion implantation samples in the range of $2\theta = 25°$ to $62°$.

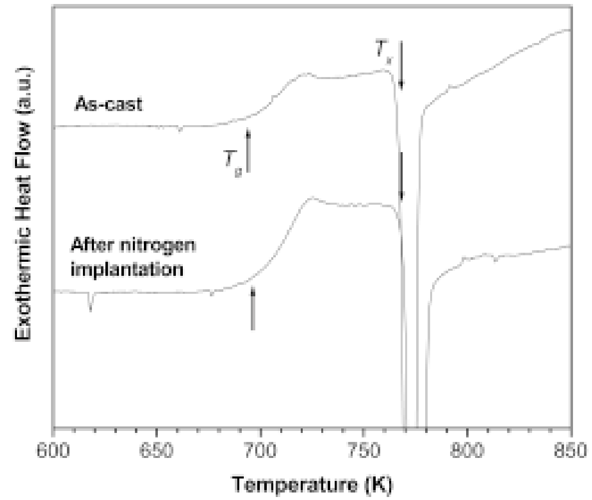

Fig. 4. DSC curves of as-cast and after nitrogen ion implanted $(Cu_{50}Zr_{50})_{92}Al_8$ samples.

tation chamber. This observation will be further investigated in XPS analysis. The penetration depth of X-ray in ZrO_2 phase is estimated to be 544 nm at grazing incidence angle of 1° with the equation:

$$x = -\ln(1-p)\cdot\left[\mu(\lambda)\cdot\left(\frac{1}{\sin\gamma}+\frac{1}{\sin(2\theta-\gamma)}\right)\right]^{-1}, \quad (1)$$

where x is the effective depth of penetration, p is the fraction of signal from the layer of interest, μ is the mass absorption coefficient and depends on the composition (in $cm^2 \cdot g^{-1}$) and the wavelength of X-ray (λ), g is the grazing incidence angle and θ is the Bragg angle. Since an amorphous diffuse peak can still be observed in the diffraction patterns of the implanted samples in Fig. 3, the thickness of the surface ZrO_2 after implantation is much less than 544 nm. This is consistent with the depth profiling results in the following.

Fig. 4 exhibits the DSC curves of the $(Cu_{50}Zr_{50})_{92}Al_8$ sample before and after nitrogen ion implantation. It can be seen that the enthalpy of crystallization (ΔH) and supercooled liquid region (ΔT_x) of the as-cast and implanted samples are more or less the same within experimental error, indicating that a large proportion of the sample remains in amorphous state after PIII treatment. It demonstrates that the amorphous structure in metallic glasses can be retained after PIII under appropriate conditions.

Fig. 5 shows the XPS depth profiles obtained from the (a) untreated control, (b) nitrogen and (c) argon ion implanted samples. The profiles have been plotted on a depth scale based on sputtering rates measured from a SiO_2 reference under similar conditions. For the no-treatment control sample, the depth profile reveals that there is only a thin layer of oxide on the surface, and the concentration of Cu and Zr are more or less the same and uniform throughout the sample. From the depth profile of the nitrogen-implanted sample, it can be clearly seen that the nitrogen depth profile resembles a Gaussian distribution, Fig. 5d. The maximum concentration of the implanted nitrogen ion is observed about 40 nm below surface. The concentration decreases gradually to 0 at.% at about 127 nm. The experimental results of N-implantation are compared with TRIM simulation [26] in Fig. 5d. Both curves fit very well to Gaussian distribution with similar level of skewness. The peak positions and widths are larger for the simulation results. This is not surprising because the sputtering rate calibration was made with a SiO_2 reference and the experimental depth values are for comparison purpose only. In view of the similar profiles

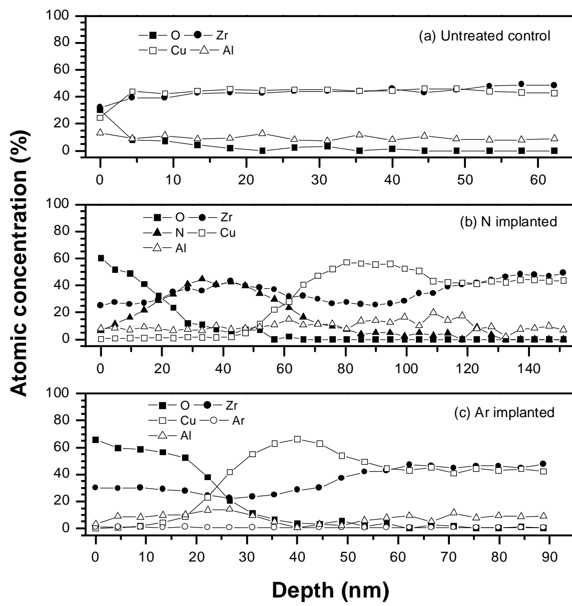

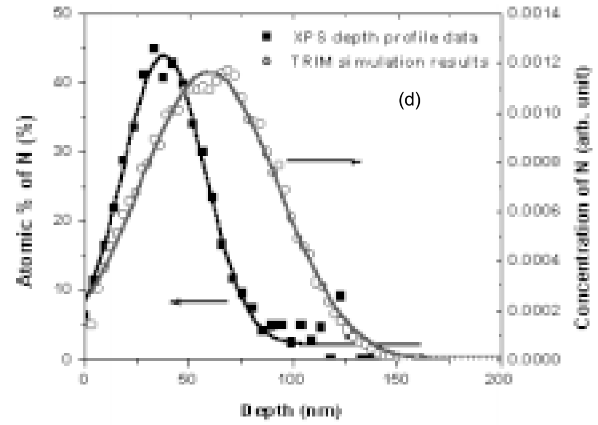

Fig. 5. XPS depth profiles of (a) untreated control, (b) nitrogen and (c) argon ion implanted $(Cu_{50}Zr_{50})_{92}Al_8$ samples. (d) A comparison of the experimental depth profile and TRIM [26] simulation results for N-implantation.

Table 1. Properties of the constituents in Cu-Zr-Al bulk metallic glass.

Element	Surface B.E. (eV) [10]	Atomic radius (Å) [10]	Electro-negativity [11]	Ionization potential (eV) [11] 1st	2nd	Oxide form	Heat of formation at 600K (kJ/mol) [12]
Cu	3.49	1.28	1.90	7.73	20.29	CuO	-154.01
						Cu_2O	-169.95
Zr	6.25	1.60	1.33	6.63	13.13	ZrO_2	-1094.97
Al	3.39	1.43	1.50	5.99	18.83	Al_2O_3	-1675.35

of the two curves, it may be concluded that there was no substantial diffusive migration of N in the BMG during the implantation process.

For the argon-implanted sample, the argon concentration is about 3 at.% throughout the profile. Since the XPS depth profiles were obtained using argon ion (Ar^+) source sputtering gun, during the sputtering process, a little portion of Ar^+ ion may be trapped into the BMG, therefore some residual argon is measured from the substrate. Only a shallow distribution of implanted argon ion was found on the top surface of the sample. This is due to the severe sputtering effect by argon ion, so that implantation is prohibited.

It is interested to note in Figs. 5b and 5c that while the concentration of Zr is nearly constant throughout the whole implanted depth, no Cu and Al was found in the topmost layer of the implanted surface. The depletion of Cu and Al is thought to be a result of selective sputtering by the plasma ion. When comparing to Zr, both Cu and Al have lower binding energies and smaller atomic sizes as shown in Table 1, they are hence easier to be knocked out from the surface by high energy plasma ions. Besides, the affinity of oxygen to different elements was one of the key factors to induce surface segregation [9]. The heat of formation of copper oxides is about –154 kJ/mol, while that of ZrO_2 is –1095 kJ/mol and Al_2O_3 is –1675 kJ/mol. Hence, the formation of Al_2O_3 is energetically preferred over that of Zr and Cu oxides. However, Al has such a low surface binding energy that Al has been knocked out from the surface. More importantly, the low concentration of Al renders the

Table 2. Peak position in experimental XPS spectra.

Element	Spectral Line	Formula	Binding energy (eV)	References
Zr	3d5/2	Zr	178.52	[15]
Zr	3d5/2	ZrO_2	183.3	[16]
Zr	3d5/2	ZrO_x	178.8	[17]
Zr	3d5/2	ZrN_x	179.9	[18]
Cu	2p3/2	Cu	932.8	[19]
Al	2p3/2	Al	72.1	[20]
Al	2p3/2	Al_2O_3	74.93	[21]
Al	2p	Al_2O_3/Al	75.6	[22]
O	1s	ZrO_2	531.23	[23]
O	1s	Al_2O_3	530.5	[24]
N	1s	N^{3-}	396.9	[25]

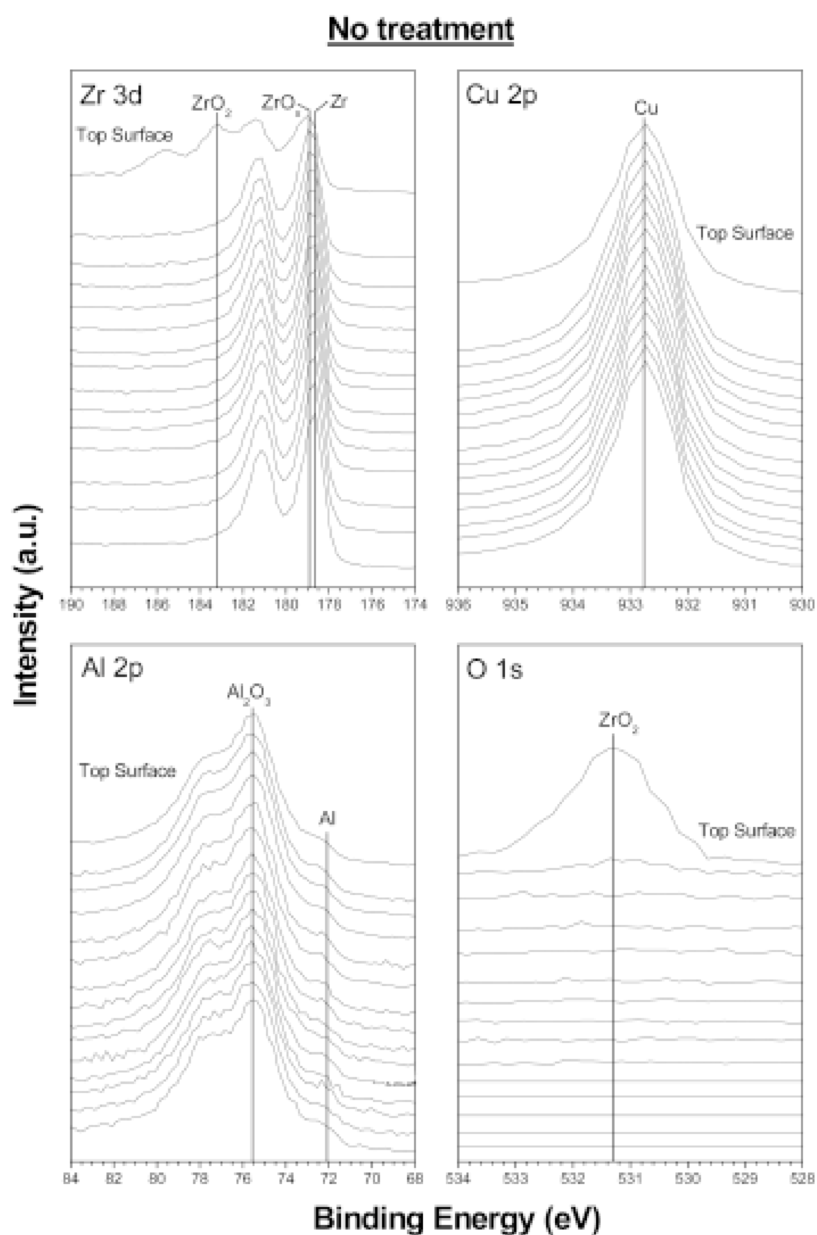

Fig. 6. XPS spectra of no treatment control $(Cu_{50}Zr_{50})_{92}Al_8$ sample.

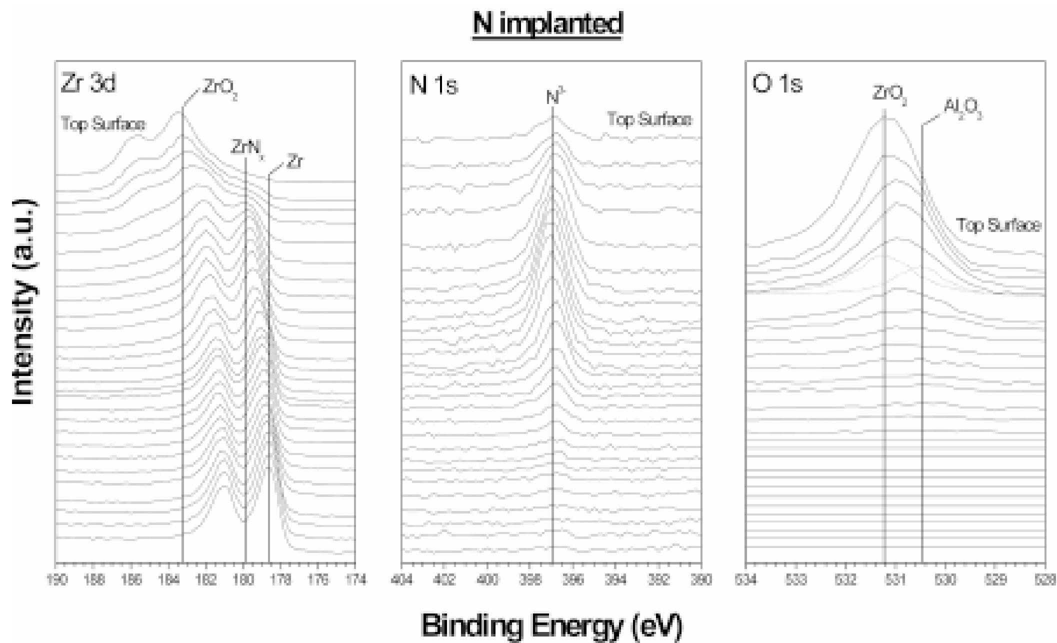

Fig. 7. XPS spectra of Zr 3d, Cu 2p3, Al 2p, N 1s and O 1s in N ion implanted $(Cu_{50}Zr_{50})_{92}Al_8$ samples. (The dotted lines are the deconvoluted ZrO_2 and Al_2O_3 peaks from the solid line using the XPSPEAK41 program).

formation of surface aluminium oxide layer difficult, hence Zr is preferentially oxidized instead of Al. This is believed to account for the suppression of Cu and Al in the implanted region [4,13,14].

Chemical states of the surface compositions in the no-treatment control and the nitrogen and argon PIII samples were studied by XPS spectra. Table 2 gives the binding energies of the elements and chemical compositions based on the XPS spectra. Their binding energies are consistent with those reported in previous studies. Fig. 6 shows the analysis of the XPS spectra of the no-treatment sample. The Zr3d spectrum reveals that the topmost layer consisted of ZrO_2 and ZrO_x, while the next 5 layers are identified as ZrO_x. Due to the abundant content of Zr, its low electronegativity and relatively low heat of formation (-1095 kJ/mol) as shown in Table 1, it is preferentially oxidized in air and form the topmost ZrO_2 layer. It is noticed from the Al2p spectra that there is a trace amount of Al_2O_3 formed throughout the sputtered layers. In the O1s spectra, the ZrO_2 peak dominates and Al_2O_3 is too weak to be detected due to its low concentration. The pre-existed Al_2O_3 may be formed in the raw material of Al with 99.9 at.% purity or formed during the casting process due to its high negative heat of formation (-1675 kJ/mol). The Cu2p spectra shows no significant binding energy shifting, indicates that Cu do not form bonding with oxygen in the no-treatment sample.

Fig. 7 displays the XPS spectra of N1s, O1s, Zr3d, Cu2p, and Al2p of the nitrogen ion implanted sample. The first layers (4.73 nm/layer for SiO_2) is identified as correspond to ZrO_2. The spectra of the subsurface layers of around 90nm thick indicate the possibility of the existence of ZrN_x in addition to ZrO_2. The energetic nitrogen ions bombard and transfer their energy to the target atoms in the sample and thus enhancing the more reactive target atoms to form bond with nitrogen ions. Comparing the electronegativities and ionization potentials (1st and 2nd) among the elements as shown in Table 1. The smaller electronegativity and ionization potential of Zr result in higher reactivity of the elements. Combining the above two factors as well as its abundant content, Zr is the most favorable element to form bonding with other elements while Cu and Al are relatively more inert. However, as no nitride is observed by GIXRD in Fig. 3, it is estimated that the amount of ZrN_x, if exists, should be small in the implanted layer. The inconsistency among the results of XPS and GIXRD may be rec-

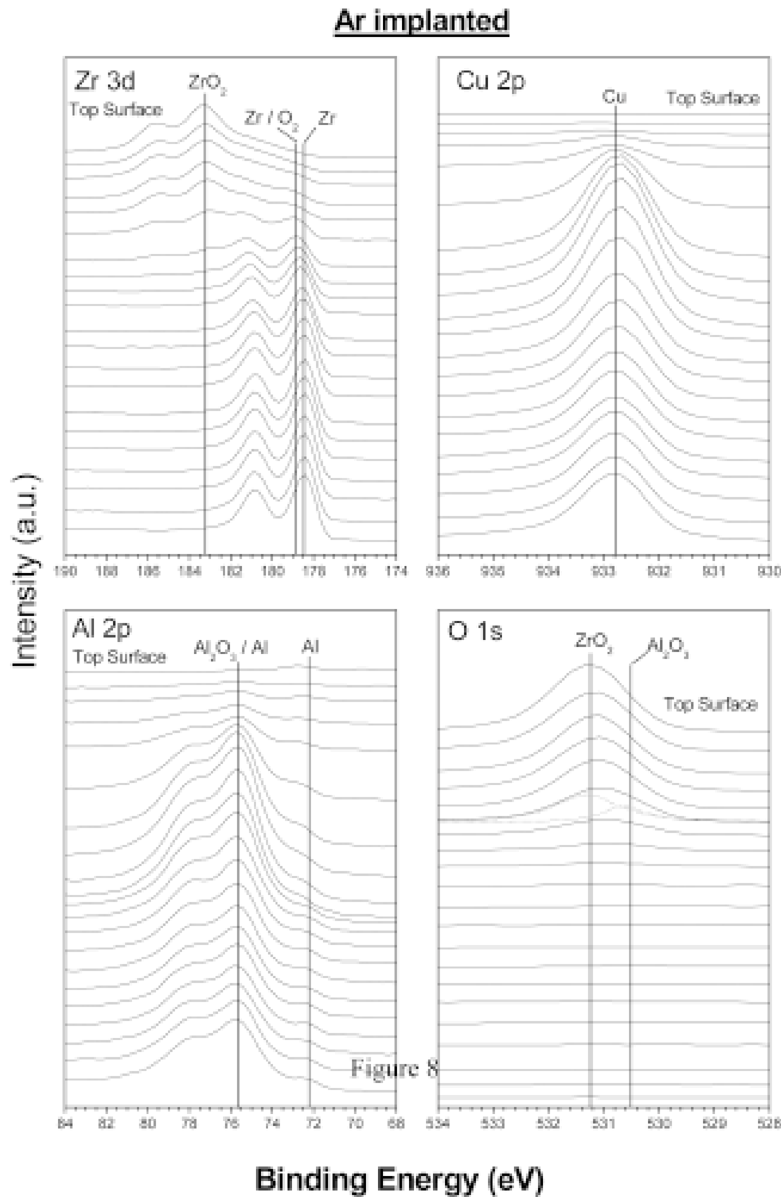

Fig. 8. XPS spectra of Zr 3d, Cu 2p3, Al 2p, Ar 2p, and O 1s in Ar ion implanted $(Cu_{50}Zr_{50})_{92}Al_8$ samples. (The dotted lines are the deconvoluted ZrO_2 and Al_2O_3 peaks from the solid line using the XPSPEAK41 program)

onciled by further experiments such as careful TEM observation to determine whether the nitrogen exists in the ZrN_x form or simply as a solute in the BMG matrix.

For the argon ion implanted sample, the XPS Zr3d spectra in Fig. 8 shows the presence of ZrO_2 on the topmost 4 layers. The next 3 sub-surface layers compose of ZrO_2 and ZrO_x, and the inner layers are ZrO_x and Zr. The purpose of designing argon PIII in metallic glass is to use the high energy argon ion (where argon is not reactive to form bonding with other elements) to bombard and transfer its energy to the 3 constituent elements in the sample, so that they form bonding among themselves and form new phases. However the XRD and XPS results show that there are no such effects. Only minor surface oxide is formed due to the inevitable oxygen contamination in the PIII instruments.

4. SUMMARY

The effect of PIII on the surface modification of $(Cu_{50}Zr_{50})_{92}Al_8$ BMG has been studied. The GIXRD curves show that the surface structure of the sample after ion implantation is crystallized, while the overall matrix remains amorphous. The XPS spectra reveal that for nitrogen and argon ion implanted samples, there is a layer of ZrO_2 formed on the surface. In the nitrogen ion implanted sample, nitrogen enrichment is observed beneath the topmost ZrO_2 layer and the nitrogen concentration depth profile resembles a Gaussian distribution. Chemical state analysis results hint that ZrN_x might have formed in the N-rich layers. Argon ion implantation has no significant effect on the composition of the sample surface. The depth profile depicts that surface segregation of Cu and Al due to the selective sputtering effects.

ACKNOWLEDGEMENTS

The authors would like to express their gratitude to Professor W.H. Wang and Mr. D.Q. Zhao, Institute of Physics, Chinese Academy of Sciences, for their assistance in the preparation of the bulk metallic glass samples. The sincere thanks are also due to Professor P.K. Chu and his group member, Department of Physics and Materials Science, City University of Hong Kong, for their kind provision of the plasma immersion ion implanter. We would express our special thanks to Professor C.M. Che, Department of Chemistry, the University of Hong Kong, who give me tremendous help in the usage of grazing incidence X-ray diffraction. The work described in this paper was fully supported by a grant from City University of Hong Kong (Strategic Research Grant, Project No. 7001991).

REFERENCES

[1] W. Zhang and A. Inoue // *Mater. Trans.* **44** (2003) 2220.

[2] S. Mandl, D. Krause, G. Thorwarth, R. Sader, F. Zeilhofer, H.H. Horch and B. Rauschenbach // *Surf. Coat. Technol.* **142-144** (2001) 1046.

[3] R.W. Y. Poon, J.P.Y. Ho, X.Y. Liu, C.Y. Chung, P.K. Chu, K.W.K. Yeung, W.W. Lu and K.M.C. Cheung // *Thin solid films* **488** (2005) 20.

[4] X.B. Tian, R.K.Y. Fu, L.W. Wang and P.K. Chu // *Mater. Sci. Eng. A* **316** (2001) 200.

[5] R.W.Y. Poon, K.W.K. Yeung, X.Y. Liu, P.K. Chu, C.Y. Chung, W.W. Lu, K.M.C. Cheung and D. Chan // *Biomaterials* **26** (2005) 2265.

[6] P. Yu, H.Y. Bai, M.B. Tang and W.L. Wang // *J. Non-Cryst. Solids* **351** (2005) 1328.

[7] T.L. Cheung and C.H. Shek, *Thermal and Mechanical Properties of Cu-Zr-Al Bulk Metallic Glasses*, In: *Proc. International Symposium on Metastable and Nano Materials 2005* (Paris, France, 3-7, July, 2005).

[8] P.K. Chu, B.Y. Tang, Y.C. Cheng and P.K. Ko // *Rev. Sci. Instruc.* **68** (1997) 1866.

[9] W.M.H. Sachtler and R.A.W. Santen // *Appl. Surf. Sci.* **3** (1979) 121.

[10] C. Kittel, *Introduction to Solid State Physics, 7th ed*. (John Wiley, New York, 1996).

[11] D.R. Lide, *CRC Handbook of Chemistry and Physics, 84th ed.* (CRC Press, BocaRaton, 2003).

[12] Barin, *Thermochemical Data of Pure Substances, 2nd ed*. (VCH, Weinheim, 1993).

[13] R.W.Y. Poon, X.Y. Liu, C.Y. Chung, P.K. Chu, K.W.K. Yeung, W.W. Lu and K.M.C. Cheung // *J. Vac. Sci. Technol. A* **23** (2005) 525.

[14] R.W.Y. Poon, J.P.Y. Ho, X.Y. Liu, C.Y. Chung, P.K. Chu, K.W.K. Yeung, W.W. Lu and K.M.C. Cheung // *Mater. Sci. Eng. A* **390** (2005) 444.

[15] C. Morant , J.M. Sanz, L. Galan and L. Soriano // *Surf. Sci.* **218** (1989) 331.

[16] Y. Baba and T.A. Sasaki // *Surf. Interface Anal.* **6** (1984) 171.

[17] L. Kumar, D.D. Sarma and S. Krummacher // *Appl. Surf. Sci.* **32** (1988) 309.

[18] I. Takano, S. Isobe, T.A. Sasaki and Y. Baba // *Appl. Surf. Sci.* **37** (1989) 25.

[19] G. Johansson, J. Hedman, A. Berndtsson, M. Klasson and R. Nilsson // *J. Electron Spectrosc. Relat. Phenom.* **2** (1973) 295.

[20] T. Kendelewicz, W.G. Petro, J.A. Silberman, I. Lindau and W.E. Spicer // *J. Vac. Sci. Technol. B* **1** (1983) 623.

[21] W.M. Mullins and B.L. Averbach // *Surf. Sci.* **206** (1988) 29.

[22] I. Olefjord, H.H. Mathieu and P. Marcus // *Surf. Interface Anal.* **15** (1990) 681.

[23] C. Morant, J.M. Sanz, L. Galan and L. Soriano // *Surf. Sci.* **218** (1989) 331.

[24] S.L.T. Andersson and M.S. Scurrell // *J. Catal.* **59** (1979) 340.

[25] Y.M. Shulg'a, V.N. Troitskii, M.I. Aivazov,Y.G and Borodk'o // *Zh. Neorg. Khimii* **21** (1976) 2621.

[26] J.F. Ziegler, J.P. Biersack and U. Littmark, *The Stopping and Range of Ions in Solids* (Pergamon Press, New York, 1984).